CEAS Space Journal (2019) 11:371–380
https://doi.org/10.1007/s12567-019-00270-y

ORIGINAL PAPER

The BepiColombo Laser Altimeter (BELA): a post-launch summary

Nicolas Thomas[1] · **Hauke Hussmann**[2] · **Luisa M. Lara**[3]

Received: 2 May 2019 / Revised: 22 July 2019 / Accepted: 29 July 2019 / Published online: 13 August 2019

Abstract
We provide a brief description of the BepiColombo Laser Altimeter experiment for the joint ESA-JAXA mission to Mercury, BepiColombo. The text describes the main elements of the instrument and discusses several of the problems encountered during the instrument development. The actions taken to mitigate the issues are also described and the resulting performance of the instrument as determined by combining ground test data with models of Mercury and the spacecraft orbit is presented. The instrument has met the requirements set in 2005 and should provide a solid data set for the global study of the topography and internal structure of Mercury.

Keywords BepiColombo · BELA · Laser altimeter

1 Introduction

The European Space Agency's BepiColombo mission to Mercury [1] was launched on 20 October 2018 from Kourou. The stack comprised two spacecraft and a transfer module. The transfer module (MTM) uses solar-electric propulsion to bring the two spacecraft to Mercury orbit. Arrival is foreseen in December 2025. The two spacecraft are the Mercury Magnetospheric Orbiter (MMO) which has been built by the Japanese space agency, JAXA and the Mercury Planetary Orbiter (MPO) which has been built by ESA.

Onboard the MPO is the first European-built laser altimeter for interplanetary flight, the BepiColombo Laser Altimeter (BELA). The instrument was selected in 2005 and the development has overcome a number of challenges in building this type of system within the given constraints. The original requirements were that the instrument should weigh < 12 kg and consume < 40 W while acquiring altimetry data at < 2 m resolution from a 400 km × 1500 km orbit on a nadir-pointed spacecraft. The final mass of the instrument was 14.2 kg and the power consumption is < 30 W in nominal operation.

This paper briefly describes the investigation, the instrument, and the test performance in the laboratory. In-flight commissioning so far suggests that the ground performance has not been modified during the launch phase.

1.1 Aims of the investigation

BepiColombo Laser Altimeter is a joint Swiss–German project with smaller involvements from Spain and France. The scientific objectives of the experiment are to measure

- the figure parameters of Mercury to establish accurate reference surfaces;
- the topographic variations relative to the reference figures and a geodetic network based on accurately measured positions of prominent topographic features;
- the tidal deformations of the surface;
- the surface roughness, local slopes and albedo variations, also in permanently shaded craters near the poles.

BELA forms an integral part of a larger geodesy and geophysics package, incorporating radio science and stereo imaging. The synergy between the instruments will allow determination of the planetary figure and gravity field, investigation of the interior structure, study of Mercury's surface morphology and geology, and possibly provide measurements of tidal deformations. The offset between the centre of

✉ Nicolas Thomas
nicolas.thomas@space.unibe.ch

1 Space Research and Planetology Division, University of Bern, Sidlerstrasse 5, 3012 Bern, Switzerland

2 German Aerospace Center, Institute of Planetary Research, Planetary Geodesy, Berlin, Germany

3 Instituto de Astrofísica de Andalucía, Granada, Spain

Table 1 Main observation types of BELA mapped to the science goals

Observation type	Goal
1	Dense global grid of range measurements between S/C and Mercury's surface to be carried out throughout the whole science mission phase
2	Measure the topography of selected morphologic features
3	Measure periodic surface deformation as a function of time (i.e., as a function of true anomaly of Mercury in its orbit around the Sun) by detecting periodic variations
4	Assist in determining Mercury's pole position and rotation rate
5	Assist in determining periodic variations of Mercury's rotation rate (physical librations)
6	Measure the albedo globally (at laser wavelength of 1064 nm) actively (with laser pulse) including in permanently shadowed regions in craters near the poles.
7	Measure the albedo (at laser wavelength of 1064 nm) passively (without laser pulse) on the sun-illuminated surface
8	Measure surface roughness globally and locally by analysing the shape of the return pulse

mass and the centre of figure will be derived. The reference surfaces and the geodetic network will provide the coordinate system for any detailed geological, physical, and chemical exploration of the surface. The topography is needed to develop digital terrain models which will allow quantitative study of the geology, tectonics, and age of the surface. The topography is further needed for a reduction of the gravity field data, because topographical contributions to gravity must first be removed before using gravity anomalies for the investigation of sub-surface structures. The use of topography together with gravity data will constrain, by an admittance analysis between the two and with the help of a flexure model for the lithosphere, both lithosphere and crust properties. Examples here would include the lithosphere elastic thickness (essential for the reconstruction of the thermal history of Mercury) and the crustal density (essential for the construction of a Hermean internal model). In addition to the moments of inertia which will be provided by the radio science experiment, the tidal deformations measured by BELA and the radio science instrument will place further constraints on global models of the interior structure. BELA will contribute by providing the deformation of the surface, while the radio science package will measure the mass concentrations. Under favourable conditions, it will even be possible to constrain the rheology of the interior of the planet by measuring the time lag between the motion of the tidal bulge and the disturbing potential.

It is to be noted that the MESSENGER Laser Altimeter (MLA) onboard NASA's MESSENGER spacecraft has provided laser altimetry data at Mercury. However, the eccentric orbit of the spacecraft resulted in good quality data being acquired only in the northern hemisphere. The southern hemisphere of Mercury is almost completely unexplored with altimetry. Hence, BELA is likely to make a major contribution to Mercury studies well beyond the MESSENGER contribution.

The main observations to be performed are itemised in Table 1.

1.2 Properties of the return pulse

Laser altimetry can provide measurements of the structure and albedo of the target surface in addition to the straightforward range measurement. If p(t) is the temporal dependence of the received number of photons in the return pulse, the three main parameters which can be extracted can be described as [2]

$$N = \int_0^\infty p(t)\, dt, \tag{1}$$

where N is the number of photons in the return pulse (a quantity related to the surface albedo).

$$T_p = \frac{1}{N} \int_0^\infty t\, p(t)\, dt, \tag{2}$$

where T_p is the pulse centroid time (a quantity related to the surface range) and

$$\sigma_p^2 = \frac{1}{N} \int_0^\infty (t - T_p)^2 p(t)\, dt, \tag{3}$$

where σ_p, is the rms pulse width (a quantity related to the surface roughness and slope). The BELA instrument is designed to obtain the range to the surface to high accuracy but also to place constraints on the surface albedo (particularly in permanently unilluminated crater bottoms at Mercury's poles) and the small scale (below 30 m) surface roughness.

2 Instrument description

2.1 Link budget

The BepiColombo Laser Altimeter was separated into two major sub-systems to allow stand-alone testing in the two main contributing countries, Switzerland and Germany.

The transmitter section of the instrument was under the responsibility of DLR and comprised the laser, its associated electronics and baffling, and the system level electronics box (incorporating the Spanish-provided power converter). The receiver section of the instrument was under the responsibility of the University of Bern and comprised the receiving optics and associated baffling, the detector and the range-finding electronics. System integration was performed at the University of Bern.

The link budget scales the laser pulse energy and the receiver aperture area. The return pulse energy at nadir can be computed using the link equation:

$$E_r = E_r T_r \frac{S}{z^2} \frac{A_N}{\pi}, \tag{4}$$

where E_r is the received pulse energy, E_t is the emitted pulse energy, T_r is the receiver optics transmission, S is the collecting area of the telescope, A_N is the target surface reflectivity and z is the altitude of the spacecraft above the surface [3, 4]. The quantity A_N/π is sometimes known as the target backscattering (coefficient) and has units of [sr^{-1}] [5]. A detailed trade-off was needed to evaluate the best configuration taking into account the size of the aperture that BELA would need to have in the thermal shield of the spacecraft. The trade-off resulted in specification of an Nd:YAG laser emitting at 1064 nm (frequency-doubling was found to be less efficient partially because of the redness of Mercury itself) operating with a nominal pulse energy of 50 mJ at 10 Hz with a 5 ns pulse duration. The aperture of the receiving telescope was 20 cm in diameter to match the required product of pulse energy and receiving aperture which is essentially the figure of merit for laser altimeter detection capability.

The link budget was computed to allow ranging from distances of up to 1055 km. This was based on the nominal orbit of MPO of 400 km × 1500 km given during Phase A. The upper limit was chosen to allow ranging over one entire hemisphere of the planet, pole-to-pole, with the argument of periherm at latitudes of < 20°. At the start of the project, when the requirements needed to be set, the gravity field of Mercury was not well established and hence the drift of the orbit with time was not at that stage predictable. The requirement and the final performance of the instrument does, however, appear to provide reasonable robustness against the orbit drift expected from observations of the gravity field [6].

2.2 The telescope

The telescope design was driven by mass and thermal constraints. Several materials were considered and rejected. Electroformed nickel was rejected because of its relatively poor thermal conductivity which would have led to distortion and loss of efficiency. Silicon carbide was considered to be too massive. An all-beryllium design was eventually chosen as a consequence of its high strength to mass ratio and good thermal properties. A fast design was chosen to reduce the overall length. The resulting telescope weighed 600 g, had a focal length of 1.25 m, and a field of view of just over 530 µrad. The field of view was again a trade-off between the background reflected light from the planet and the need to align and maintain the alignment of the outgoing laser pulse with the receiver field of view when the instrument was placed under thermal load. The telescope comprised a parabolic primary and a hyperbolic secondary. The imaging quality is not good but this is, of course irrelevant, because the instrument requires light collection and filtering and not 2-D imaging.

2.3 Filtering background radiation

The instrument operates over both the nightside and the dayside. Over the dayside, the reflected light from the surface of Mercury is, of course, large and hence a narrow-band interference filter was incorporated into the design. The width of the filter was a delicate trade-off. The temperature inside the spacecraft and at the instrument was expected to be between roughly − 30 and + 55 °C depending upon the position of Mercury about the Sun (Mercury has a relatively high orbital eccentricity which produces a strongly varying heat load on the spacecraft) and the errors in the spacecraft thermal model. Variations in temperature affect both the laser emission wavelength (~ 4.85 pm/K) and the bandpass of interference filters (~ 8 pm/K). It was, therefore, necessary to select a bandwidth about the Nd:YAG wavelength that was both large enough to cope with the temperature variations at both positions in the instrument and yet narrow enough to eliminate most of the reflected sunlight from the surface. A value of 1.7 nm for the bandwidth was selected.

It was decided to place the filter behind the Cassegrain focus of the telescope in a 1:1 transfer optic to ensure the beam was parallel when passing through the filter. The back-end optics are, however, asymmetric about the filter to allow better straylight control.

2.4 The detector

The detector is an infrared enhanced silicon avalanche photodiode (APD) from Excelitas (formerly Perkin-Elmer). This device, which was based on the C30954E APD, has flown in several laser altimeters built by Goddard Space Flight Center for interplanetary flight including the MESSENGER Laser Altimeter (MLA), the Lunar Orbiter Laser Altimeter

(LOLA) and the Mars Orbiter Laser Altimeter (MOLA). The device has a quantum efficiency of 34% at 1064 nm making it ideal for this application. The active surface is around in 800 µm diameter. It should be noted that the sensitivity of the device is not uniform at high gains and, therefore, centering of the returned beam on the APD is of considerable importance. The APD requires a high voltage source which is provided by a separate analogue electronics board.

A Peltier element was added to the APD packaging to allow thermal control. In normal mode, the APD temperature can be set between 0 and 25 °C. The optimum signal to noise is a fairly complex trade-off between detection efficiency and dark current. Originally, the plan was to reduce the dark current by selecting lower temperatures. However, testing illustrated that the optimum signal to noise has a rather broad maximum and higher temperatures may actually be preferable. The Peltier can also be used to heat to > 60 °C to allow for the possibility of in-flight annealing of radiation damage.

2.5 Detection scheme

Unlike previous interplanetary altimeters, a digital detection scheme was selected (rather than analogue detection). This was only feasible because of the recent availability of fast radiation tolerant ADCs. At the time of selection, it was possible to use two phase-shifted 40 MHz ADCs thereby obtaining 12.5 ns sampling of the return pulse which, when combined with the two-way light time, gives a vertical resolution of 1.875 m. A range window is used to limit the number of samples obtained. The length of the range window at maximum is equivalent to a distance range of 30 km which is sufficient to cover the expected topographic height variation and the error in the spacecraft position. The approximate altitude of the spacecraft can be passed to the instrument for rapid initialisation of ranging.

The digital detection scheme (a proprietary firmware from Thales Alenia Space Switzerland) allows fitting of the return pulse with a range window at 10 Hz frequency using arbitrary pulse shapes. This fitting of the return pulse has been shown to provide resolutions up to a factor of 8 higher in optimum signal-to-noise conditions. The pulse shapes can be programmed by telecommand using two free parameters to define the final curve. The scheme can also search for the best fit using four different families of pulse shapes within one range window read-out. Depending upon the telemetry (downlink) allocation, one can, therefore, return only the information for the best fit, the information for up to four peaks in the range window, or the entire range window if required for ground analysis of the returned pulse shape. Flexibility has also been incorporated to allow combinations of these modes. A mode that has been used frequently for testing is a multi-mode, where the results for pulse families have been returned but for every tenth shot (i.e., every 1 s), the full range window has been returned.

2.6 The laser and beam expander

The laser for BELA has been fully described by Kallenbach et al. [7]. It comprises two main elements. The laser head box (LHB) contains a primary and a redundant, single-stage, actively q-switched, diode laser side-pumped Nd:YAG rod laser system with unstable resonator geometry. Each of the two Nd:YAG laser rods inside the LHB is pumped by four laser diode assemblies (LDAs) manufactured by semiconductor devices (SCD) emitting at 808 nm wavelength with an electrical-to-optical efficiency. The LDAs are driven by 100 A diode laser current pulses with 200 µs supplied from a 300 V capacitor reservoir (Fig. 2, right). A 3 kV voltage across a Pockels' cell is switched to actively open the optical path in the laser resonator for stimulation of laser radiation at 1064 nm. The optical-to-optical efficiency for the conversion of the pump light into the laser radiation is about 10%. To extract the stored energy at this high efficiency, the q-switch needs to transit from non-polarizing to quarter-wavelength condition in < 30 ns. To protect the laser optics from laser-induced damage effects and limit outgassing effects, the LHB is pressurized with synthetic air and sealed by C-rings when prevent a pressure drop of more than 100 mbars over a 12-year mission time (this mission duration requirement was set to include a possible extended mission and margin. The current nominal mission duration is slightly under 8 years). The beam expander (BEX) optics narrows the beam divergence to 60 µrad and is integrated into the LHB. This reduction of the footprint size allows a smaller field of view for the receiver and hence limits background reflected light. This sub-element comprises three lenses and a sapphire window between the first and second lens through which the laser beam exits the pressurized LHB volume.

Given the dangerous nature of the laser, a (red tag) safety plug was implemented to prevent unexpected/unintentional firing.

2.7 The time of flight measurement

Within the laser head box, a small mirror extracts a part of the outgoing pulse and passes it to a redundant pair of optical fibres than bring the light to the focal plane of the receiver. The switching of the Q-switch is not known precisely enough to provide a good estimate of the time of the outgoing pulse (Q-switching is used to produce nanosecond pulses and is achieved by putting a variable attenuator inside the laser's optical resonator. When the attenuator is functioning, light which leaves the gain medium does not return, and lasing cannot begin. Removing the attenuator initiates lasing). But it is well enough known such that the receiver

chain can be active and waiting for the light to arrive out of the optical fibre. The use of the same detection chain for the outgoing and incoming pulses eliminates a large number of issues in calibrating the time delays within the instrument itself. After the start pulse is initiated, the instrument sets the range window for the return pulse and completes the time flight measurement with respect to its 80 MHz clock that is calibrated against the spacecraft pulse per second tick (PPS). The calibration of the spacecraft PPS from ground is, therefore, an additional measurement needed independent of the instrument itself.

2.8 Baffling and thermal control

At Mercury, a 20 cm aperture can allow up to 300 W of direct sunlight into the instrument and the spacecraft. This was an extreme challenge for the design of the instrument. The approach adopted was similar to an idea developed by Thales Alenia Space Switzerland (then Oerlikon) in the frame of an ESA study called LAPE (Laser Altimeter for Planetary Exploration). A reflective baffle (RBU), constructed from a combination of ellipsoidal and hyperbolic surfaces, was produced following a patent by Stavroudis [8]. The length of the baffle and the number of vanes is specified by the minimum angle the Sun reaches with respect to the optical axis of the instrument. In the case of BepiColombo, Mercury itself occults the Sun for angles up to 38° from the boresight. The original idea was to maximize the reflectance of the baffle using interference coatings. However, the challenges of depositing uniform thin layers on hyperbolic-shaped substrates was shown to be critical and a polished aluminium solution reduced risk while only slightly compromising the performance (Fig. 1). Modelling showed that solar photons from > 38° off-axis would be rejected by the baffle after 1.4 bounces (on average). It was also shown that 90% of the power entering the baffle would be rejected resulting in a heating of the baffle with around 30 W.

Difficulties were encountered when attempting to use standard thermal modelling software to determine temperatures, because the shapes of the surfaces could not be defined accurately enough within the software environment. Detailed analyses were necessary to model the baffles and to correlate the test results [9, 10].

The external surface (where the baffle slightly protrudes above the spacecraft panel) was protected with a ceramic ring. Testing, using a dedicated simulator producing a wide, parallel beam equivalent to 7 solar constants [11], indicated that this ring would reach over 200 °C. Thermal decoupling of the elements from the rest of the instrument was required. The heat from the baffle itself could be dumped into the spacecraft through a support bracket and effectively solved the thermal issues with the receiver.

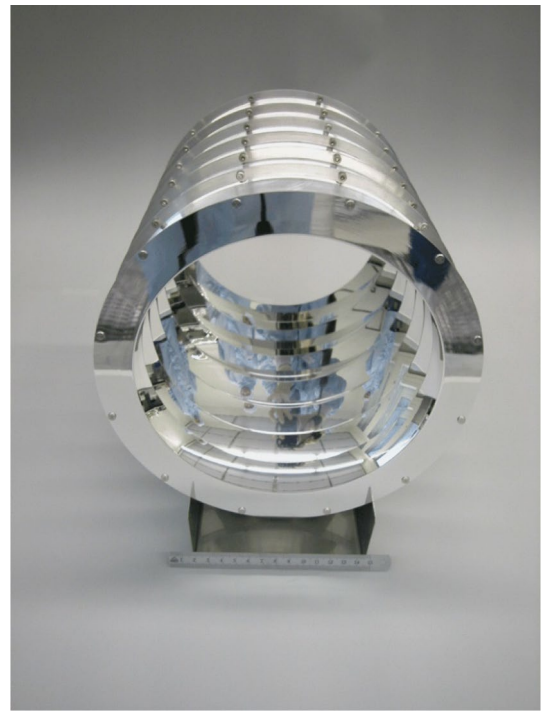

Fig. 1 Prototype version of the receiver baffle. Note the reflection of the photographer seen in the baffle vanes. The prototype (inner diameter = 204 mm) was 719 g

The laser was also baffled (using the transmitter baffle unit, TBU) to prevent light striking the sensitive lens surfaces. The baffle structure was similar but smaller because of the smaller aperture. However, an additional sleeve-like baffle (the SPU) was also included to limit contamination of the coated front lens.

2.9 The electronics unit

An electronics unit (ELU) houses the rangefinder module (RFM), the digital control module (DCM) and the Spanish-provided power converter module (PCM). The DCM runs a primary boot software that is used to initialise the instrument and take over low level functions of BELA (including operational heaters). An application software (APS) that performs higher level commanding and control can then be started. The APS allows control of the acquisition mode and can also be used to diagnose issues in a diagnostic mode.

2.10 Summary of BELA units

BepiColombo Laser Altimeter comprises seven individual units, as indicated in Table 2.

Table 2 Summary of the BELA units mounted to the spacecraft and their purposes

Unit	Acronym	Purpose
Electronics Unit	ELU	The ELU contains the Digital Processing Module (DPM), the PCM (power converter module) and the RFM (Rangefinder module, i.e., the digital part of the rangefinder electronics) in one box. This box has the only direct electrical interface to the S/C
Laser Electronics Unit	LEU	The LEU controls the laser and provides the laser with power (dedicated power converter)
Transmitter Baffle Unit	TBU	The TBU has no mechanical or thermal (conductive) connection to any other part of BELA, but is mounted directly to a dedicated support bracket, provided by the S/C. It prevents sunlight reaching the beam expander and the laser head box
Straylight & Contamination Protection Unit	SPU	The SPU is mounted on the S/C optical bench and closes the gap between the transmitter aperture (the beam expander last surface) and the TBU and provides protection against contamination and straylight
Receiver Baffle Unit	RBU	The RBU limits the absorption of direct sunlight entering the receiver aperture. It has no mechanical or thermal (conductive) connection to any other part of BELA. It is mounted directly to a dedicated support bracket, provided by the S/C
Analogue Electronics Unit	AEU	An electronics box which contains a high voltage (< 500 V) source (HVS) for the APD, and proximity electronics for the rangefinder (analogue electronics)
Baseplate Unit	BPU	The BPU comprises a baseplate upon which other elements are mounted the receiver telescope (RTL) the Rx Focal Plane Assembly (FPA), which includes the Back-End Optics (BEO) (which itself includes an interference filter for isolating the 1064 nm laser light), the avalanche photo-diode (APD) detector the laser head box (LHB) incl. the beam expander required to produce the required footprint diameter. Two optical fibres take a fraction of the emitted pulse to the Rx FPA to support detection of the time of the emitted pulse

2.11 Basic operational approach

When BELA is initialised, it has no knowledge of the spacecraft's position with respect to the target surface. Two methods of starting ranging have been foreseen. Firstly, the spacecraft can pass an estimate of the altitude above the surface and the rate of change of altitude to the instrument. The accuracy of this estimate should be of the order of 30 km so that the pulse can be expected within the range window. In general, ESA's flight dynamics can easily achieve this accuracy. The second method is that BELA can scan from 300 km to 1600 km range until it finds a stable return. The first method (using a "known" value to initialise the instrument) should be seen as a backup solution in case of low signal to noise and/or scanning failure.

Once the instrument has found the return pulse, it tracks the pulse and can begin to narrow the range window. Narrowing the range window reduces the chances of the onboard algorithm being perturbed by noise. Tables within the instrument can also be used to modify instrument parameters (e.g., the gain) as the distance to the surface changes. This allows the user to optimize the instrument for high, low, or intermediate signal-to-noise cases.

The figure of merit that we have used for BELA is the probability of false detection (PFD)—the probability that the instrument returns a range that is not that of the actual pulse but that of a noise spike within the range window. The minimization of the PFD has been the main goal of the instrument development and forms our main performance criterion. It should be noted that PFDs of up to 90% (in BELA's case this would be 1 good range measurement every second on average) can still provide scientifically useful data.

The nominal pulse frequency is 10 Hz but operational frequencies can be reduced to limit either data volume and/or power consumption. Nominal data rates can be up to ~ 10 kbps at 10 Hz with an enhanced mode at 12.5 kbps. This can, however, be reduced substantially if the minimum continuous frequency of 1 Hz is used.

If the laser fails at some point in the mission, the instrument can still be used in Albedo Mode, where the APD is used to determine the albedo of the surface within the FOV at 1064 nm as a passive radiometer using a low data rate (256 bps).

3 Performance results

Several issues were encountered during the instrument development and we look here at three items that caused considerable concern prior to delivery, their resolution, and the resulting performance.

3.1 Major issues encountered

3.1.1 Control of laser noise

As can be imagined, the charging of the laser and the sudden release of the energy using the Pockels' cell can generate

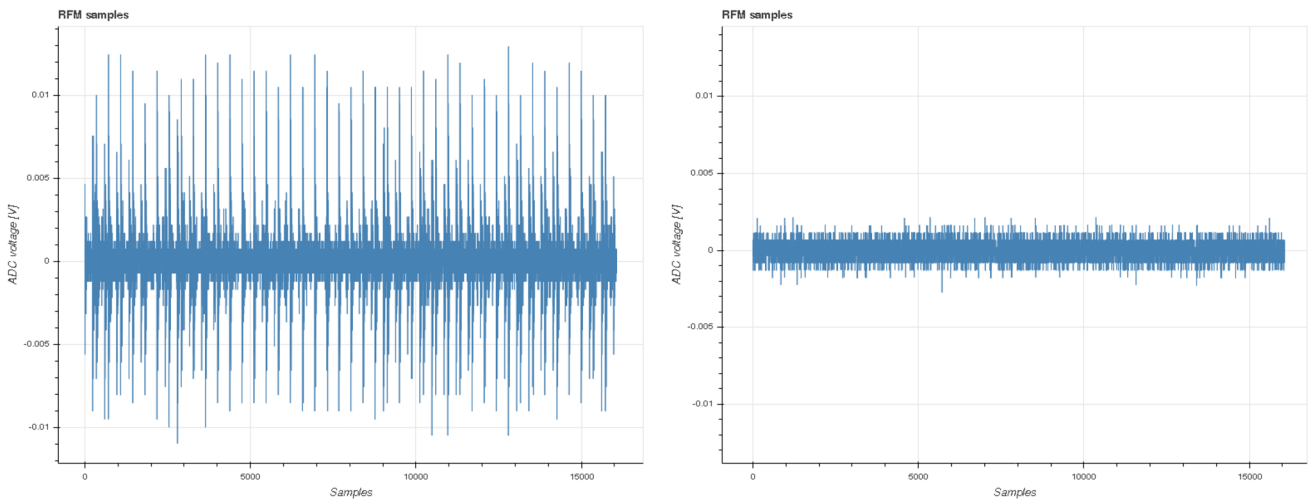

Fig. 2 Noise in the receiver chain before (left) and after (right) application of the noise mitigation measures

significant noise in the electronics. This noise source is very close to a highly sensitive detection chain that is attempting to pick-out the signal from 200 to 500 photons striking the detector. Three strong sources of electronic distortions are active with the APD operating with a noise floor of about 0.3 pA $Hz^{-1/2}$ [12]. Firstly, the current pulses driving the pump diodes form one source. Secondly, the emission of the 50 mJ pulses is actively triggered by a voltage ramp of 3 kV with 30 ns rise time applied to thr Pockels' cell crystal. The maximum current supplied by the Pockels' cell driver (PCD) circuit reaches values of about 3 A to load the required 30 pF within 30 ns. Finally, the fly-back converter which continuously charges the 40 µF capacitor reservoir of the laser diode driver (LDD). Its pulse width modulator (PWM) switches up to 1 A load current with a repetition rate of about 220 kHz. The influence on the detection chain of these distortions was underestimated in the original design and results of early testing on, what was subsequently realised to be non-representative prototypes, led to a need to take counter-measures relatively late in the programme. It was also recognized that the grounding concept adopted on the spacecraft was not ideal [12], leading to noise getting to the detector chain not merely through the common mode ground but also through the instrument structure. A solution using PI filters (Glenair) was found and its effectiveness is illustrated in Fig. 2 which shows the noise characteristics of the detector chain before (left) and after (right) implementation of the PI filters on the flight unit.

3.1.2 Electrostatic discharge

A further significant problem that was also encountered relatively late in the programme was repeated failure of the detector on the flight model during receiver integration. While the root cause was not fully established, several preventive measures were implemented. Of these, two are noteworthy. Firstly, a socket, made of ultra high molecular weight polyethylene (UHMW-PE), used to protect the detector from neutron radiation was removed. This socket was thought to be a potential source of (partial) electrostatic discharge and indeed, while the analysis of damage to the APD was not conclusive, this seems a prime candidate. Hence, it was removed from the system. A second measure was the reduction of the bias voltage to be applied to the APD. HV operation too close to APD breakdown can result in damage to the device. While evidence of this as a root failure mechanism was not confirmed, it was recommended the operational voltage of the HV APD input from about 370 V (30 V below breakdown) to about 340 V (60 V below breakdown) at 25 °C. This latter measure has influence on the performance as it reduced the effective gain of the APD from 1.5 MV/W to 0.75 MV/W. This value can, however, be set by the flight software. We, therefore, provide signal-to-noise calculations in the form of a probability of false detection at both values of gain.

3.1.3 Temperature stability

One of the major design issues was to ensure that the transmitter and the receiver remain aligned under thermal load. The use of isostatic mounts was intended to support this. The alignment in air at ambient temperature was performed using a system that did not require any changes in setup when switching between the receiver and transmitter for positioning [13]. However, there were residuals expected when the instrument was placed under thermal load and a special setup was prepared to measure the co-alignment over

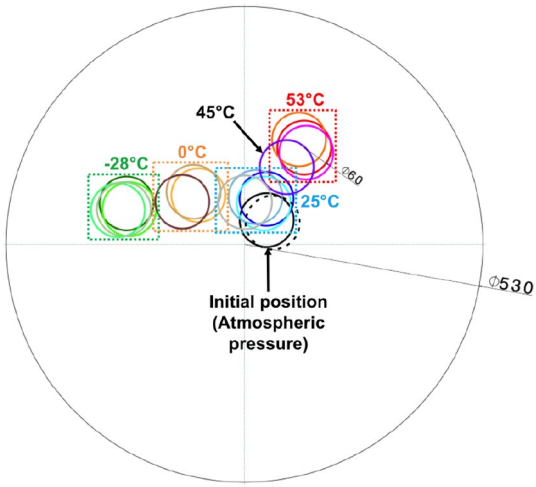

Fig. 3 Co-alignment of the transmitter and the receiver over a range of temperature. The field of view of the receiver is shown as the large circle. The small circles are to scale and show the footprint of the laser spot. The diagram shows that the laser spot stays with the receiver field of view over the full temperature range expected

in yellow. The figure shows that without the noise mitigation errors, BELA would not have reached its objectives. However, the performance with noise mitigation and high gain offers the prospect of being able to range over most of the nominal orbit, thereby exceeding requirement. It should be mentioned, however, that these values are beginning of life and some degradation is to be expected. On the other hand this could also be compensated by increasing the laser pulse energy at the cost of higher net power consumption (and probably reduced lifetime as a result of increased stress on the pump diode).

If a Gaussian type return pulse is assumed (e.g., for a lava plain on the surface), sub-sampling and fitting can result in very high accuracy for the instrument alone with values approaching 20 cm vertical accuracy being feasible in high signal-to-noise cases. However, the errors in the ranging arising from spacecraft pointing uncertainty can result in far larger errors with 10 m range error being possible for 15–20 µrad spacecraft pointing uncertainty. One of the major contributors to this error is the thermal stability of the spacecraft panel upon which BELA is mounted. Calibration

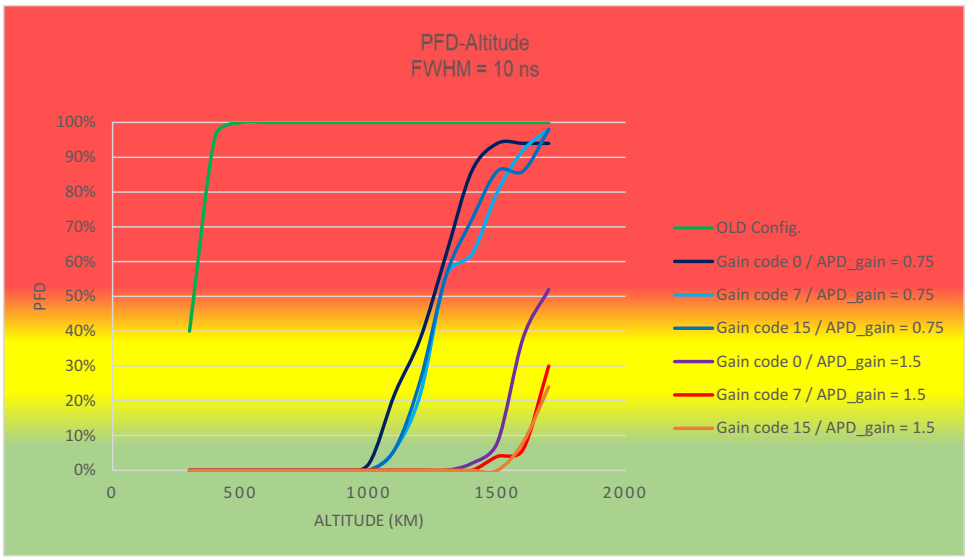

Fig. 4 PFD for different BELA configurations as a function of altitude above the surface. The pre-noise mitigation values are given in green. The different detection chain gain codes and the APD gains provide slightly different results discussed in the text. The colour coded background indicates excellent performance in green, moderate performance in yellow and poorer performance in red

a wide range of temperature [14]. The result for the flight unit is shown in Fig. 3.

3.2 Final detection capability

The final detection capability using our figure of merit, the PFD, is shown in Fig. 4. This (rather colourful) diagram shows how the instrument performs with different gain settings for the APD as well as showing the performance with the "old" configuration before the noise mitigation measures were implemented. Poor PFD values are in the red section of the diagram and good ones in green and to a lesser extent

of this error is feasible in principle using multiple observations of crater crossing combined with camera observations. However, this is an intensive task requiring careful simulation and at this stage it is not yet clear what the ultimate accuracy from such an approach might be.

Integration of laser altimeter measurements into the Bernese GNSS modelling software [15] has been initiated. Modelling with this software suggests that pointing uncertainty is now the major error source in the chain (this will be discussed further in a PhD thesis to be completed later this year).

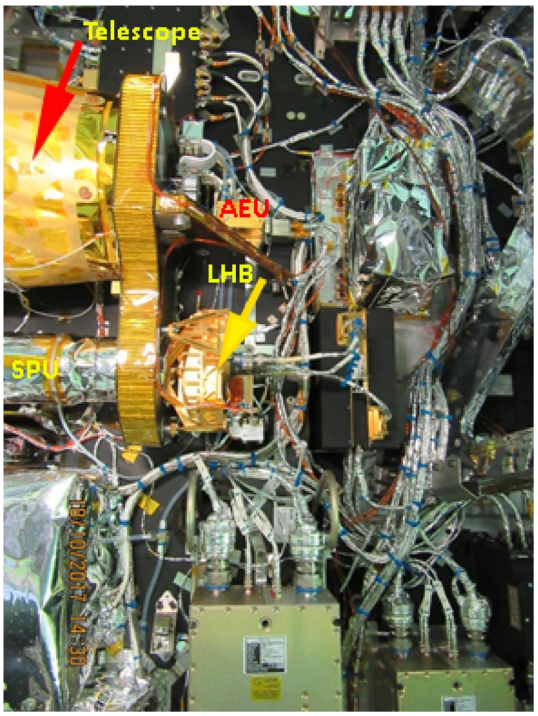

Fig. 5 BELA instrument on the spacecraft. The baffles can be seen on the left (upper) part of the image. The yellow side of the aluminium honeycomb baseplate is also evident. The laser head box is just to the right of the baseplate

For the albedo measurements, the accuracy is expected to be no better than 20% on average because of poor definition of the wings of the return pulse in low signal-to-noise cases.

For the surface roughness, low roughness terrains will be poorly defined because of the bandwidth filtering used to increase the signal to noise for the range measurement. However, very rough terrains will provide wider return pulses and, in good signal-to-noise cases, should allow identification of areas unsuitable for any future landed missions.

Figure 5 shows the BELA instrument on the spacecraft.

4 Future prospects

At the time of writing, BepiColombo is on its way to its first gravity assist on a 7-year flight to Mercury. The BELA instrument has undergone a first commissioning that demonstrated that the electronics had successfully survived launch.

Unfortunately, on the spacecraft, the transfer module of the composite spacecraft is in front of BELA. If the laser fires against the spacecraft, back reflections are potentially damaging and hence test firings are forbidden until transfer module separation in December 2025. Hence, a full shakedown of BELA will only occur when in Mercury orbit. After this, however, we expect BELA to provide a high quality data set. A more positive aspect of being behind the transfer module during cruise is that radiation damage of the detector and the laser is expected to be minimized. Consequently, the system should exhibit laser pulse energies and receiver noise characteristics similar to those observed on ground during the initial operational phase.

Over the first 176 days, BELA will map the surface to provide a global map of the surface topography. Subsequent observations will be used to fill-in gaps and to provide additional information on the tidal flexing of the planet. The first global map will probably be computed from ground tracks separated by around 25 km at the equator. Filling in should improve this with time. To facilitate this, the spacecraft can roll by $\pm 5°$ to optimize the data acquisition. At 10 Hz, the ground-track pulse spacing will be typically 300 m allowing good definition of crater structures and scarps over the whole planet. The orbit is polar, and therefore, we will pass over the poles every orbit. This is ideal for investigation of the unilluminated interiors of polar craters that may conceal bright water ice.

While the polar orbit gives good coverage, the spacecraft orbit reconstruction (and, therefore, the accuracy of the topography) is dramatically improved by crossing ground tracks. In a true polar orbit, this only occurs at the two poles. But using the roll of the spacecraft the latitude of the crossings can be reduced. Although this is still not optimum, it is an improvement and also forms part of our operational concept. Combining these possibilities we expect BELA to achieve its goals and provide high quality results.

Acknowledgements BELA is a joint Swiss–German project with the participation of Spain. We gratefully acknowledge financial support from the Swiss Space Office via ESA's PRODEX programme, the German Aerospace Center's Space Administration, the Ministerio de Ciencia e Innovación, and the Ministerio de Economía y Competitividad.

References

1. Benkhoff, J., van Casteren, J., Hayakawa, H., Fujimoto, M., Laakso, H., Novara, M., Ferri, P., Middleton, H.R., Ziethe, R.: BepiColombo comprehensive exploration of Mercury: mission overview and science goals. Planet. Space Sci. **58**, 2–20 (2010)
2. Gardner, C.S.: Ranging performance of satellite laser altimeters. Proc. IEEE **30**(5), 1061–1072 (1992)
3. Zuber, M.T., Smith, D.E., Solomon, S.C., Muhleman, D.O., Head, J.W., Garvin, J.B., Abshire, J.B., Bufton, J.L.: J. Geophys. Res. **97**(E5), 7781–7797 (1992)
4. Abshire, J.B., Sun, X., Afzal, R.S.: Mars Orbiter Laser Altimeter: receiver model and performance analysis. Appl. Opt. **39**(15), 2449–2460 (2000)
5. Bufton, J.L.: Laser altimetry measurements from aircraft and spacecraft. Proc. IEEE **77**(3), 463–477 (1989)
6. Smith, D.E., Zuber, M.T., Phillips, R.J., Solomon, S.C., Hauck II, S.A., Lemoine, F.G., Mazarico, E., Neumann, G.A., Peale, S.J., Margot, J.-L., Johnson, C.L., Torrence, M.H., Perry, M.E., Rowlands, D.D., Goossens, S., Head, J.W., Taylor, A.H.: Gravity field

and internal structure of Mercury from MESSENGER. Science **336**, 214 (2012)
7. Kallenbach, R., Murphy, E., Gramkow, B., Rech, M., Weidlich, K., Leikert, T., Henkelmann, R., Trefzger, B., Metz, B., Michaelis, H., Lingenauber, K., DelTogno, S., Behnke, T., Thomas, N., Piazza, D., Seiferlin, K.: Space-qualified laser system for the BepiColombo Laser Altimeter. Appl. Opt. **52**, 8732 (2013)
8. Seiferlin, K., Chakraborty, S., Gunderson, K., Fischer, J., Lüthi, B., Piazza, D., Rieder, M., Sigrist, M., Thomas, N., Weigel, T.: Design and manufacture of a lightweight reflective baffle for the BepiColombo Laser Altimeter. Opt. Eng. **46**, 043003 (2007)
9. Beck, T., Lüthi, B., Messina, G., Piazza, D., Seiferlin, K., Thomas, N.: Thermal analysis of a reflective baffle designed for space applications. Acta Astronaut. **69**, 323–334 (2011)
10. Beck, T., Bieler, A., Thomas, N.: Numerical thermal mathematical model correlation to thermal balance test using adaptive particle swarm optimisation (APSO). Appl. Therm. Eng. **38**, 168–174 (2012)
11. Thomas, N., Beck, T., Chakraborty, S., Gerber, M., Graf, S., Piazza, D., Roethlisberger, G.: A wide-beam solar simulator for simulating the solar flux at the orbit of Mercury. Meas. Sci. Technol. **22**, 065903 (2011)
12. Kallenbach, R., Behnke, T., Perplies, H., Henkelmann, R., Rech, M., Geissbuhler, U., Peteut, A., Lichopoj, A., Schroedter, R., Michaelis, H., Seiferlin, K., Thomas, N., Castro, J.M., Herranz, M., Lara, L.: Electromagnetic compatibility of transmitter, receiver, and communication port of a space-qualified laser altimeter. ESA Workshop on Aerospace EMS **738**, 54 (2016)
13. Chakraborty, S., Affolter, M., Gunderson, K., Neubert, J., Thomas, N., Beck, T., Gerber, M., Graf, S., Piazza, D., Pommerol, A., Roethlisberger, G., Seiferlin, K.: High accuracy alignment facility for the receiver and transmitter of the BepiColombo Laser Altimeter. Appl. Opt. **51**, 4907 (2012)
14. Gouman, J., Beck, T., Affolter, M., Thomas, N., Geissbühler, U., Peteut, A., Bandy, T., Servonet, A., Piazza, D., Seiferlin, K., Ghose, K.: Measurement and stability of the pointing of the BepiColombo Laser Altimeter under thermal load. Acta Astronaut. **105**, 171–180 (2014)
15. Dach, R., Lutz, S., Walser, P., Fridez, P. (Eds.) (2015) Bernese GNSS Software Version 5.2. Documentation, Astronomical Institute, University of Bern, Bern. ISBN: 78-3-906813-05-9. https://doi.org/10.7892/boris.72297